A polarization-diversity wavelength duplexer circuit in silicon-on-insulator photonic wires

Wim Bogaerts, Dirk Taillaert, Pieter Dumon, Dries Van Thourhout, Roel Baets

Ghent University - Interuniversity Microelectronics Center (IMEC), Department of Information Technology
Sint-Pietersnieuwstraat 41, 9000 Gent, Belgium
wim.bogaerts@intec.ugent.be

http://photonics.intec.ugent.be

Elroy Pluk

Genexis B.V.
Lodewijkstraat 1a, 5652 AC Eindhoven, The Netherlands

Abstract: We present a wavelength duplexer based on a compact arrayed waveguide grating (AWG) in silicon-on-insulator (SOI) photonic wire waveguides. Polarization insensitive operation is achieved through a special polarization diversity approach in which we use 2-D grating fiber couplers as integrated polarization splitters. To mitigate the effects of process variations, we propagated both polarizations in opposite directions through the same AWG with a mere $600 \times 350\,\mu m^2$ footprint. This resulted in an on-chip insertion loss between $-2.1\,dB$ and $-6.9\,dB$, crosstalk of $-15\,dB$, and only $0.66\,dB$ polarization dependent loss. This is the first demonstration of a functional polarization-diversity circuit implemented in SOI nanophotonic waveguides, including interfaces to single-mode fiber.

OCIS codes: (130.0130) Integrated Optics; (130.1750) Components; (230.3120) Integrated Optics Devices

References and links

1. W. Bogaerts, P. Dumon, D. Van Thourhout, D. Taillaert, P. Jaenen, J. Wouters, B. S., V. Wiaux, and R. Baets, "Compact Wavelength-Selective Functions in Silicon-on-Insulator Photonic Wires," J. Sel. Top. Quantum Electron. **12**(6), 1394–1401 (2006).
2. C. Gunn, "Silicon photonics - Poised to invade local area networks," Photonics Spectra **40**(3), 62–68 (2006).
3. W. Bogaerts, R. Baets, P. Dumon, V. Wiaux, S. Beckx, D. Taillaert, B. Luyssaert, J. Van Campenhout, P. Bienstman, and D. Van Thourhout, "Nanophotonic Waveguides in Silicon-on-Insulator fabricated with CMOS technology," J. Lightwave Technol. **23**(1), 401–412 (2005).
4. P. Dumon, W. Bogaerts, V. Wiaux, J. Wouters, S. Beckx, J. Van Campenhout, D. Taillaert, B. Luyssaert, P. Bienstman, D. Van Thourhout, and R. Baets, "Low-loss SOI photonic wires and ring resonators fabricated with deep UV Lithography," IEEE Photon. Technol. Lett. **16**(5), 1328–1330 (2004).
5. G. Reed, G. Mashanovich, W. Headley, B. Timotijevic, F. Gardes, S. Chan, P. Waugh, N. Emerson, C. Png, M. Paniccia, A. Liu, D. Hak, and V. Passaro, "Issues associated with polarization independence in Silicon Photonics," J. Sel. Top. Quantum Electron. **12**(6), 1335–1344 (2006).
6. C. Doerr, M. Zimgibl, C. Joyner, L. Stultz, and H. Presby, "Polarization diversity Waveguide Grating Receiver with Integrated Optical Amplifiers," IEEE Photon. Technol. Lett. **9**, 85 (1997).

#78792 - $15.00 USD Received 8 January 2007; revised 9 February 2007; accepted 9 February 2007

7. T. Barwicz, M. Watts, M. Popovic, P. Rakich, L. Socci, F. Kartner, E. Ippen, and H. Smith, "Polarization-transparent microphotonic devices in the strong confinement limit," Nature Photonics **1**, 57–60 (2007).
8. D. Taillaert, H. Chong, P. Borel, L. Frandsen, R. De La Rue, and R. Baets, "A compact two-dimensional grating coupler used as a polarization splitter," IEEE Photon Technol. Lett. **15**(9), 1249–1251 (2003).
9. D. Taillaert and R. Baets, "Fiber-to-waveguide coupler," US Patent 7,065,272 B2 (2005).
10. P. Urban, E. Pluk, E. Klein, A. Koonen, G. Khoe, and H. de Waardt, "Simulation Results of dynamically reconfigurable Broadband Photonic Access Networks (BB Photonics)," in *2nd IET International Conference on Access Technologies (ICAT)*, p. 93 (Cambridge, UK, 2006).
11. R. Roy, G. Manhoudt, C. Roeloffzen, and W. van Etten, "Control and management scheme in a DWDM EPON," in *Proceedings of the 8th International Conference on Transparent Optical Networks (ICTON)*, p. Tu.D1.6 (Nottingham, UK, 2006).
12. D. Taillaert, P. Bienstman, and R. Baets, "Compact efficient broadband grating coupler for silicon-on-insulator waveguides," Opt. Lett. **29**(23), 2749–2751 (2004).
13. W. Bogaerts, D. Taillaert, B. Luyssaert, P. Dumon, J. Van Campenhout, P. Bienstman, D. Van Thourhout, R. Baets, V. Wiaux, and S. Beckx, "Basic structures for photonic integrated circuits in Silicon-on-insulator," Opt. Express **12**(8), 1583–1591 (2004).
14. D. Taillaert, W. Bogaerts, P. Bienstman, T. Krauss, P. Van Daele, I. Moerman, S. Verstuyft, K. De Mesel, and R. Baets, "An out-of-plane grating coupler for efficient butt-coupling between compact planar waveguides and single-mode fibers," J. Quantum Electron. **38**(7), 949–955 (2002).
15. T. Tsuchizawa, K. Yamada, H. Fukuda, T. Watanabe, J. Takahashi, M. Takahashi, T. Shoji, E. Tamechika, S. Itabashi, and H. Morita, "Microphotonics devices based on silicon microfabrication technology," IEEE J. Sel. Top. Quantum Electron. **11**(1), 232–240 (2005).
16. K. Sasaki, F. Ohno, A. Motegi, and T. Baba, "Arrayed waveguide grating of $70 \times 60\ \mu m^2$ size based on Si photonic wire waveguides," Electron. Lett. **41**(14), 801–802 (2005).
17. P. Dumon, W. Bogaerts, D. Van Thourhout, D. Taillaert, R. Baets, J. Wouters, S. Beckx, and P. Jaenen, "Compact wavelength router based on a Silicon-on-insulator arrayed waveguide grating pigtailed to a fiber array," Opt. Express **14**(2), 664–669 (2006).
18. C. R. Doerr, "Planar Lightwave Devices for WDM," in *Optical Fiber Telecommunications*, I. P. Kaminow and T. Li, eds., vol. IV A, chap. 9, pp. 405 – 476 (Academic Press, ISBN 0-12-395172-0, 2002).
19. D. Dai and S. He, "Accurate two-dimensional model of an arrayed-waveguide grating demultiplexer and optimal design based on the reciprocity theory," J. Opt. Soc. Am. A **21**(12), 2392–2398 (2004).
20. Y. Barbarin, X. Leijtens, E. Bente, L. C.M., K. J.R., and M. Smit, "Extremely small AWG demultiplexer fabricated on InP by using a double-etch process," IEEE Photon. Technol. Lett. **16**(11), 2478–2480 (2004).
21. Y. Hida, Y. Hibino, M. Itoh, A. Sugita, A. Himeno, and Y. Ohmori, "Fabrication of low-loss and polarisation-insensitive 256 channel arrayed-waveguide grating with 25 GHz spacing using 1.5%Δ waveguides," Electron. Lett. **36**(9), 820–821 (2000).
22. Y. Hibino, "Recent advances in high-density and large-scale AWG multi/demultiplexers with higher index-contrast silica-based PLCs," J. Lightwave Technol. **8**(6), 1090–1101 (2002).

1. Introduction

Silicon-on-insulator (SOI) photonic wires are very well suited to implement wavelength-selective functions in a very compact way [1, 2, 3]. The high-contrast, submicron waveguides allow for very tight bends and close packing of components on a photonic integrated circuit. This could lead to both larger-scale integration and more complex but inexpensive components. These are exactly the requirements for components in large-scale deployment of optical access networks, as used in fiber-to-the-home. Photonic wires with losses as low as $2.5 dB/cm$ have already been demonstrated fabricated with industrial CMOS fabrication tools [4, 3]. However, there are still a number of obstacles for the widespread application of this technology. The high refractive index contrast and wavelength-scale dimensions make photonic wires inherently polarization dependent, so circuits will only work for a single polarization. But in standard single-mode fiber the polarization is an unknown and variable quantity. While photonic wires with a square cross section embedded in silica are in principle polarization independent, they are very intolerant to small variations in the geometry of the waveguide cross section, making them difficult to fabricate. In addition, polarization-independent design of functional building blocks, like directional couplers or ring resonators, is not trivial and sometimes even impossible [5]. In our solution, we avoid the issue of polarization independent waveguides by

#78792 - $15.00 USD Received 8 January 2007; revised 9 February 2007; accepted 9 February 2007

using a single-polarization photonic wire circuit in a polarization-diversity scheme: We split the polarization in the fiber into two orthogonal polarizations which can be processed in separate circuits [6, 7]. This way, polarization-independent operation can be achieved. However, for wavelength-selective operation it is of the utmost importance that the circuits for both polarizations functions identically. In high-contrast nanophotonics, this requires either an extreme accuracy in fabrication or the use of local active tuning.

Here, we present the first demonstration of an application-oriented, functional polarization-diversity circuit based on a compact 2-D fiber coupler grating, which also functions as a polarization splitter [8, 9]. This allows us to implement a wavelength duplexer for a low-cost fiber access network using a very compact arrayed waveguide grating (AWG). To ensure polarization independence, we designed the circuits in such a way that both polarizations make use of the same wavelength-selective element by traveling through the AWG in opposite directions. This results in a polarization dependent loss (PDL) of only $0.66\,dB$.

In section 2 we discuss the specifications of the wavelength duplexer in terms of transmission spectrum. We then discuss the design of two critical aspects of the polarization-diversity approach in section 3: The 2-D fiber coupler and the bidirectional AWG. The spectral design of the AWG is covered in more detail in section 4. Section 5 describes the fabrication with CMOS technology, as well as the transmission measurements. The performance in terms of polarization diversity is discussed in section 6, and we try to give a qualitative insight on how to improve the device even further.

2. Wavelength duplexer

In many of today's fiber-to-the-home (FTTH) systems two different wavelengths are used for upstream and downstream traffic. These wavelengths are often widely separated, being positioned around $1310\,nm$ and $1550\,nm$, respectively. However, a growing trend is to use wavelength division multiplexing (WDM) over passive optical networks (PON). Here, it is possible to use multiple wavelengths for multiple subscribers over the same fiber, allowing for more flexible expansion of the networks without the need to install more optical fiber. It is important to note that while the subscribers transmit and receive on different wavelengths, for economical reasons they should all use the same transceiver module. This module should therefore be wavelength-independent for all upstream and all downstream wavelengths. Therefore, often reflective modulation is used, e.g. by a reflective semiconductor optical amplifier (RSOA) as illustrated in Fig. 1. This device can then modulate a downstream-traveling CW carrier, eliminating the need for a tunable source at the subscriber side. The subscriber wavelengths can then easily be allocated from the central office [10, 11]. Modulation speeds are relatively low, with mainstream users requiring a mere $100Mbps$-$1Gbps$.

A possible choice for the upstream and downstream wavelengths is to have them grouped in two wider wavelength bands. In our case, the design criteria dictate two $400\,GHz$ bands, each containing $8 \times 50\,GHz$ channels, with a band separation of $150\,GHz$. For this purpose, we designed a wavelength duplexer using an arrayed waveguide grating.

3. Designing a polarization diversity circuit

The main challenge for making a polarization independent circuit with polarization dependent waveguides is that the unknown fiber polarization should be converted to a specific waveguide polarization. In a polarization diversity approach, the unknown fiber polarization is decomposed into two orthogonal polarizations. For this purpose, we use a 2-D periodic fiber coupler grating. Each polarization can then be processed in its own single-polarization circuit.

When using such a polarization diversity scheme, the difficulty is to ensure that both circuits function identically. For wavelength-selective functions, this requires very accurate fabrication,

#78792 - $15.00 USD Received 8 January 2007; revised 9 February 2007; accepted 9 February 2007

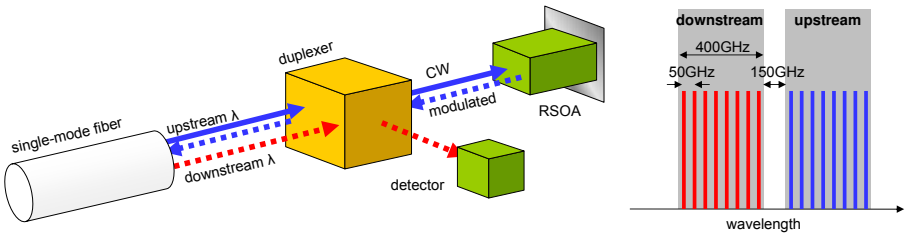

Fig. 1. Principle of duplexer-based fiber access end-point. The downstream and upstream operate each on one 50 *GHz*-spaced ITU channel within a 400 *GHz* band. By using a reflective approach, the channel can be selected at the central office.

which in high-contrast systems (like SOI) need to be of the order of 1 *nm* or better. This is much stricter than the precision required for high-end CMOS fabrication. The tolerances become only manageable when using a somewhat lower index contrast, like in SiN waveguides, in combination with tightly-controlled e-beam lithography [7].

3.1. 2-D fiber couplers for polarization splitting

To use polarization dependent photonic wires in a polarization-diversity scheme, the random fiber polarizations should be split into its constituent linear polarizations. Fiber couplers gratings, as now often used for SOI nanophotonic circuits, typically work for a single fiber polarization [12]. However, a 2-D periodic grating can couple both fiber polarizations to the TE-mode of their own photonic wire waveguide [8, 13]. This way, the grating coupler doubles as a polarization splitter, making a polarization diversity approach possible by processing both fiber polarizations in their own circuit. As both fiber polarizations are coupled to the TE-mode of the waveguide, no additional on-chip TE/TM polarization conversion is needed, like in [7].

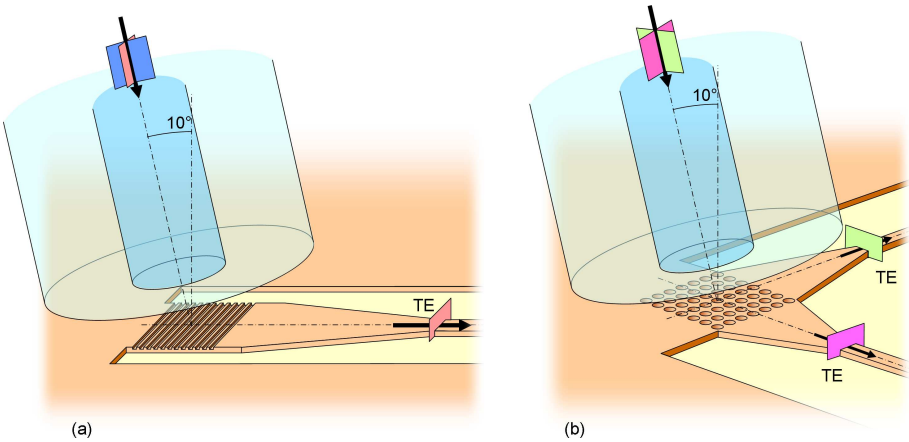

Fig. 2. Principle of the 2-D fiber coupler with integrated polarization splitter. (a) 1-D grating coupler for TE-polarization. (b) 2-D grating coupler which decomposes the fiber polarizations into two linear polarizations which are coupled to the TE-modes of both waveguides.

Figure 2(a) shows the principle of the grating fiber coupler [14]. The fiber is positioned vertically over the grating. The second-order grating is optimized to couple TE-polarized light from the fiber into a 10μm broad waveguide. The fiber is tilted at a 10° angle. This allows for slightly detuned grating, avoiding second-order reflections back into the waveguide [12].

#78792 - $15.00 USD Received 8 January 2007; revised 9 February 2007; accepted 9 February 2007

The 2-D fiber coupler, first introduced in Ref. [8], is an extremely compact way to integrate a fiber-to-waveguide interface and a polarization splitter/combiner. In a first approximation it can be seen as a superposition of two 1-D fiber couplers, like in Fig. 2(b). The 2-D grating decomposes the fiber polarization into two linear polarizations, and each gets coupled to a $10\mu m$ broad ridge waveguide. For a vertical fibre a genuine second-order grating can be used, and the on-chip waveguides are at right angles with the fiber and with each other. However, as shown in [8], this can generate a cavity response in the waveguide, because the grating has strong second-order reflections. As a solution, we propose here to detune the 2-D grating to avoid reflections in the waveguides. This again results in a tilted fiber with a 10° angle to the vertical. As a consequence, the on-chip waveguides are no longer at 90° with respect to each other, but angled inward at 3.1°.

The 2-D grating has a period of $605nm$, and the circular holes have a diameter of $390nm$. The waveguides of the fiber coupler are etched through the silicon top layer, but the grating holes are only etched $70nm$ deep. This can be seen in the fabricated device, shown further in Fig. 7.

3.2. Bidirectional use of an AWG

To ensure polarization independence when using this approach, the circuits for both polarizations should function identically. For wavelength-selective functions implemented in a high-contrast system like SOI this requires very accurate fabrication technology. Typically, to assure a $50\,GHz$-accuracy ($0.4\,nm$) in channel positioning, the dimensions of the waveguide should be controlled substantially better than $1\,nm$. Even though we use advanced CMOS processing for the fabrication, the reproducibility and uniformity is insufficient to guarantee this accuracy. Spectrally aligning two separate circuits be solved with local active tuning mechanisms, but this would dramatically increase the complexity of the device.

We solved this problem by propagating both fiber polarizations through the same circuit but in opposite direction. In an AWG, the critical element that controls the channel spacing is the array of delay lines. We designed the AWG such that both polarizations could use the same set of delay lines. The principle of this setup is shown in Fig. 3. The two orthogonal fiber polarizations are indicated with P_1 and P_2. As shown here, we have not yet added the detector and RSOA, but used the same type of 2-D fiber couplers to combine the polarizations at the output ports to easily characterize them.

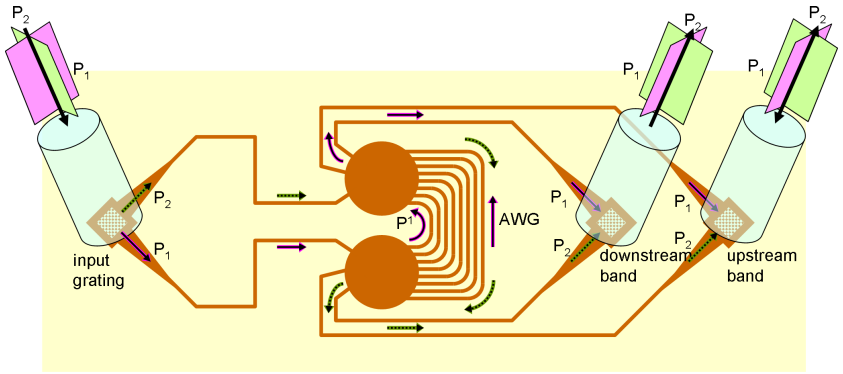

Fig. 3. Principle of a polarization independent duplexer using a polarization splitting grating coupler and bidirectional propagation through an AWG. Both fiber polarizations P_1 and P_2 travel through the same set of grating arms in opposite direction. At the output the polarizations can be recombined again with 2-D grating couplers.

#78792 - $15.00 USD Received 8 January 2007; revised 9 February 2007; accepted 9 February 2007

4. Design of the AWG

It has been shown by various groups that it is possible to implement very compact wavelength-selective functions using SOI photonic wires [1, 15]. AWGs in this technology have also been demonstrated, but with more crosstalk and less uniformity than in low index-contrast materials [16, 17]. The main challenge of the device presented here is the definition of the two broad $400\,GHz$ wavelength bands with a relatively small $150\,GHz$ channel spacing, an acceptable uniformity within the wavelength band ($5\,dB$) and sufficiently low crosstalk ($-15\,dB$). Also, the AWG has to allow for bidirectional propagation, so the input port for one fiber polarization should not physically overlap with the output ports of the other polarization.

For the design of the AWG we adapted known techniques for the simulation of AWGs [18] to be used with the high refractive index contrast of SOI. We simulated the star couplers by expanding the input mode at the interface with the Free Propagation Region (FPR) into plane waves (or rather, slab modes), propagating these to the other side of the star coupler in the direction of a given arrayed waveguide, and adding the plane waves back together. The obtained field is then overlapped with the arrayed waveguide field in order to obtain the transmission through the star coupler. This method avoids using a Fraunhofer approximation, which is necessary as due to the wide diffraction angle in high-index contrast systems, paraxiality does not hold for the entire structure. This simulation method is basically two-dimensional, approximating the vertical dimension in the FPR through an effective index method. However, for high index contrast systems the choice of the waveguide fields becomes critical, as both the mode tails and the discontinuities at the interface between core and cladding are not well approximated by an effective index method. Therefore, a horizontal cross section of the real (3-D) mode profile is used, resulting in an acceptable representation of both the mode tails and the high spatial-frequency components. Alternatively one can use the 3-D mode profile and take the overlap with the slab mode [19]. Finally, a matrix multiplication is used to calculate the full AWG, taking into account both amplitude and phase of the star coupler transmission.

When designing an AWG with one output port for each wavelength band, as is suggested in Fig. 3, it turns out to be extremely difficult to meet all criteria at the same time. When designing for low crosstalk, with a steep roll-off, the uniformity for the wavelength channels at the edges of each band is too low, and vice versa. Techniques for attaining a flat transmission band have not been proven in such high refractive index contrast.

We have solved this by combining two AWG ports for each wavelength band. This results in a total of 4 output ports for each polarization. We started our design with a uniform spacing of the ports of $275\,GHz$, calculated from the design criteria as $275\,GHz = (400\,GHz + 150\,GHz)/2$, to get a symmetric transmission spectrum in the desired wavelength bands, as shown in Fig. 4(a). Then we shifted the position of ports at the interface with the FPR, effectively moving the port wavelengths closer together [Fig. 4(b)]. This way, we got the transmission spectrum of the four ports to form two wavelength bands with the desired properties, as in Fig. 4(c). For this device, we did not yet combine the signals in the port pairs on-chip, instead we directed all four individual outputs to 2-D fiber couplers. In the final device, it is planned to add the signal powers electrically. However, it should also be possible to use a symmetric Y-splitter at each port to combine the port pairs optically. The result of both techniques is illustrated in Fig. 4(c). While combining the signals optically would increase the insertion loss at the peaks of the bands, it would also improve the intra-band uniformity.

To allow for bidirectional propagation, we had to make sure that input and output ports are well separated at the interface with the FPR. Therefore, we shifted the input and output ports with respect to the centerline of the free propagation region, making sure there is sufficient spacing between the input aperture and the output apertures. The resulting structure is shown in Fig. 5(b).To increase coupling efficiency at the interface with the FPR of the AWG, the lateral

#78792 - $15.00 USD Received 8 January 2007; revised 9 February 2007; accepted 9 February 2007

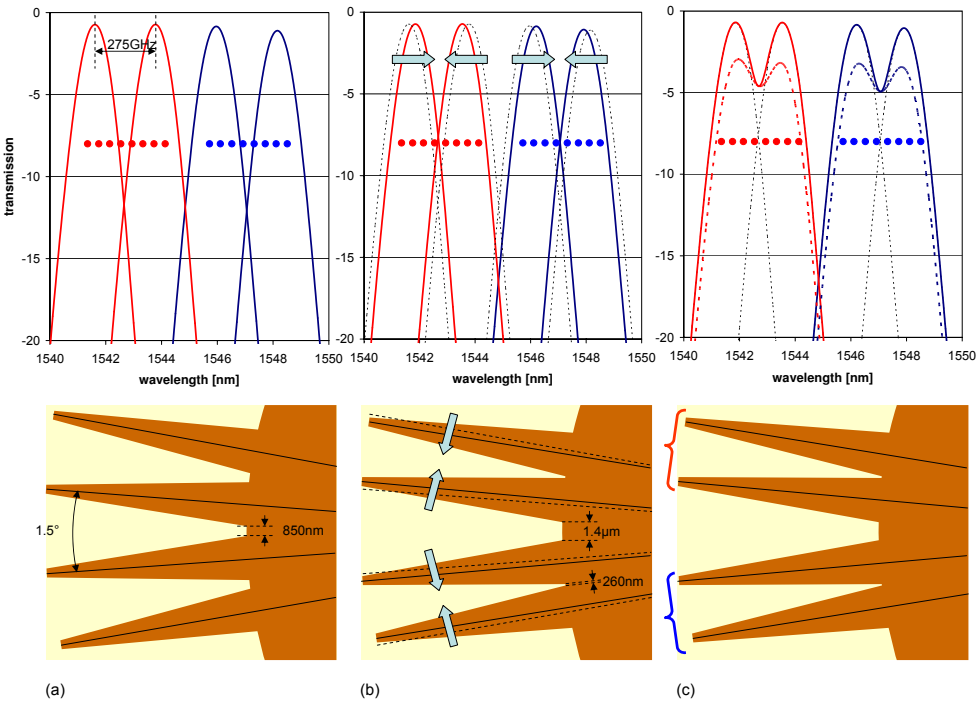

Fig. 4. Design of the AWG. (a) The transmission of the AWG output ports when located at their original channel spacings of 275 GHz. (b) The output ports are shifted towards each other in pairs. (c) When the signals in the ports are added up, two broad wavelength bands form. Full line: signals combined electrically (power); dashed line: signals combined using a lossless symmetric Y-junction.

index contrast was lowered locally by using a two-step etch process [17, 20]. Near the access ports, the waveguides are etched only 70 nm into the silicon instead of the full 220 nm. This is shown in Fig. 5(a).

The resulting AWG, shown in Fig. 6, has 48 arrayed waveguides and occupies a 600 $\mu m \times$ 350 μm footprint. The nominal channel spacing of the AWG is 275 GHz, with a free spectral range of 3.85 THz. To reduce phase errors in the delay lines due to fabrication fluctuations, we have broadened the straight sections of the delay lines to 800 nm [1, 17]. Because these broader waveguides are multi-mode, they are narrowed down at the bends with 3 μm bend radius to their single-mode width of 500 nm using a 3 μm long taper.

5. Fabrication and results

We fabricated the duplexer chip on 200 mm SOI wafers using CMOS-compatible processes on industrial tools. The SOI layer stack consists of a 220 nm silicon and 2 μm buried oxide. Patterning was done using 248 nm Deep UV lithography [3]. The etching was done using ICP-RIE etching. First, a shallow etch of 70 nm is used for the AWG star couplers and the 2-D fiber couplers. Next, the waveguides are defined using a deep etch through the SOI core layer. Alignment accuracy between the two lithography steps is of the order of 50 nm. The fabricated device is shown in Fig. 6.

The device was characterized by measuring the transmission of a broadband LED source with an optical spectrum analyzer. Both are connected to standard single-mode fiber, which is

#78792 - $15.00 USD Received 8 January 2007; revised 9 February 2007; accepted 9 February 2007

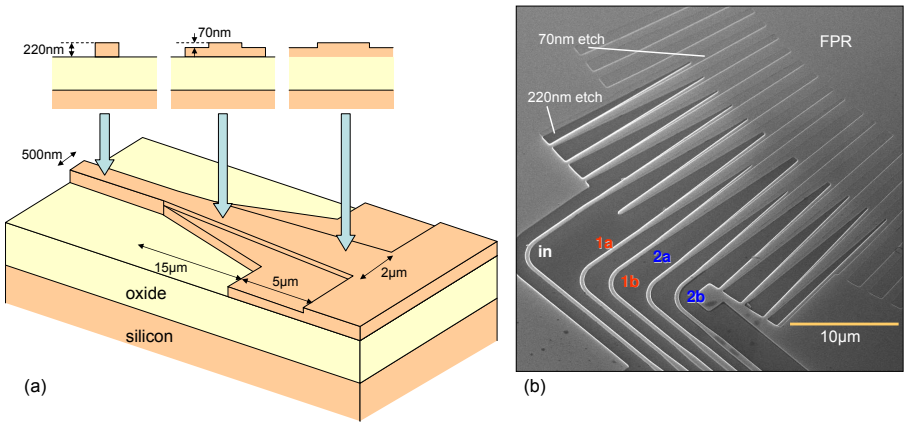

Fig. 5. Interface with the free propagation region (FPR) of the AWG. (a) Near the interface, the access waveguides transition from deep etch to shallow etch to reduce reflections. (b) The fabricated structure shows the double etch scheme and the shifted ports.

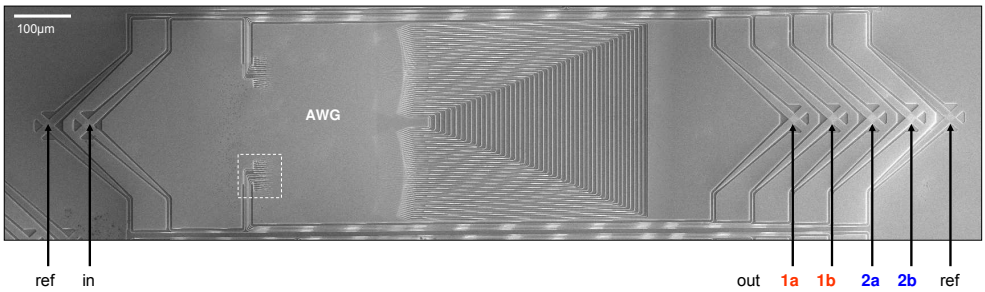

Fig. 6. SEM of fabricated duplexer. The outermost fiber couplers are directly connected and are used for as alignment and reference. The AWG has a $600 \times 350\,\mu m^2$ footprint. The two outputs for each wavelength band are not grouped but characterized individually.

compatible with the 2-D grating couplers. The fiber grating couplers consist of a 2-D periodic lattice of etched holes, with a period of $605\,nm$ and a hole diameter of $390\,nm$, etched $70\,nm$ deep, as shown in Fig. 7(b). The single-mode fiber hovers over the grating at a 10° angle with the vertical. Figure 7a shows the coupling spectrum of a single 2-D grating coupler. This loss per coupler was extracted from the transmission of a reference waveguide, which directly connects two 2-D fiber couplers (see Fig. 6). The efficiency for a single fiber-to-chip coupling has a Gaussian wavelength dependence, which translates in a parabolic profile when expressed in dB, as in Fig. 7. The optimal efficiency is 21% ($-6.7\,dB$ coupling loss), with a $3\,dB$ bandwidth of $60\,nm$. This coupling efficiency is lower than reported efficiencies of 1-D fiber couplers, which only function for a single polarization [2, 12], but it should be noted that for this device we used an etch depth optimized for these 1-D gratings, and not for the 2-D gratings. The transmission spectrum of the 2-D fiber couplers also exhibit much less fringes as in [8], because of the detuning of the grating and the slight tilt of the fiber.

Figure 8 shows the transmission of the four AWG ports normalized to the reference waveguide. In the final device, the four AWG output channels will be combined in pairs into two $400\,GHz$ wavelength bands indicated in Fig. 8. We have also plotted the original design values for these two bands, and we can see that while the shape of the transmission band matches

#78792 - $15.00 USD Received 8 January 2007; revised 9 February 2007; accepted 9 February 2007

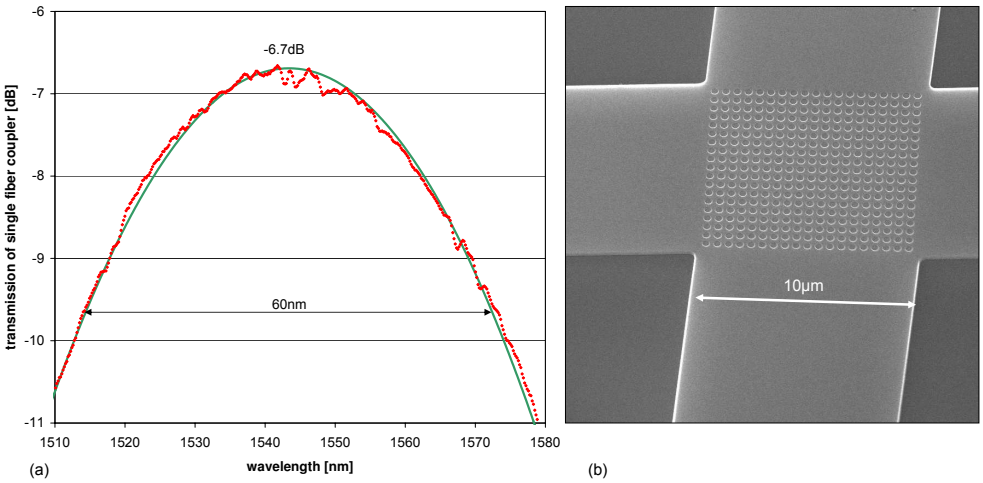

Fig. 7. 2-D grating fiber couplers: (a) Transmission of a single coupler, extracted from the transmission of the reference waveguide. (b) an SEM picture of the fiber coupler and access waveguides.

very well the design, there is a wavelength shift of more than $10\,nm$, more than can be compensated for with simple thermal tuning. However, this can be entirely attributed to the fact that the waveguides in the fabricated structures are broader than in the original design. Using broader waveguides drastically reduces the phase errors caused by fluctuations in waveguide geometry [1]. During lithography, we can artificially broaden the waveguides with respect to their design value by illuminating with a lower energy dose. In this case, underexposure broadened the (already broad by design) wires in the delay lines from $800\,nm$ to $900\,nm$. When using these values instead of the design values, the simulated transmission matches the experimental results very well. Non-uniformity within the combined wavelength bands is $4.8\,dB$, resulting in an insertion loss between $-2.1\,dB$ and $-6.9\,dB$. This is only $1.5\,dB$ worse than the original design value. Crosstalk between the bands is as low as $-15\,dB$.

6. Polarization dependence

6.1. Measurements

To measure polarization dependence, we observed the output power while randomly varying the input polarization. This was done by applying torque on the input fiber with polarization control wheels. When using the partially polarized LED, we observed no fluctuations in the transmission spectrum, either in power or in the position and shape of the transmission peaks.

To get a more accurate measure of the polarization dependent loss (PDL), we repeated the exercise using a highly polarized tunable laser. Figure 9 shows the power fluctuation over time, at a constant wavelength $\lambda = \lambda_1$ near the peak of port 2a, indicated in Fig. 8. We chose this point in the transmission spectrum because it should be rather sensitive to polarization dependence in the circuit. In the first 20 seconds, we did not alter the polarization. Then, the polarization was ramdomly changed by rotating the polarization controller wheels. While the power fluctuates stronger, we measured a polarization dependent loss (PDL) of only $0.66\,dB$. This is better than the $1.5\,dB$ of similar semiconductor polarization-diversity devices [6], and of the same order as the PDL of low-contrast integrated components [21, 22] or SiN circuits [7] .

#78792 - $15.00 USD Received 8 January 2007; revised 9 February 2007; accepted 9 February 2007

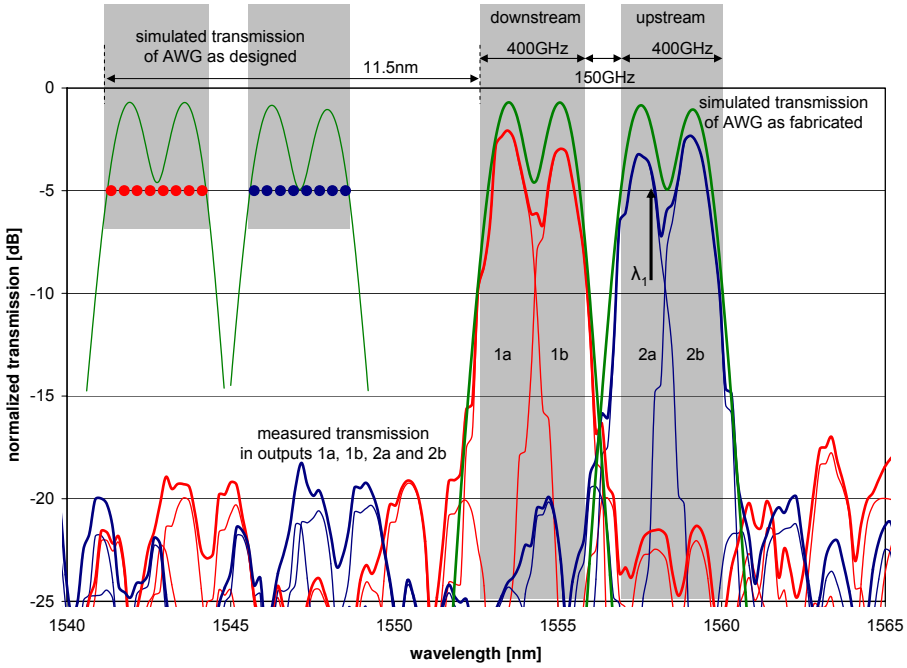

Fig. 8. Transmission of the duplexer output ports indicated in Fig. 6 normalized to the transmission of the grating couplers in Fig. 7. The original design simulation is also indicated, as well as the simulated transmission of the fabricated structure

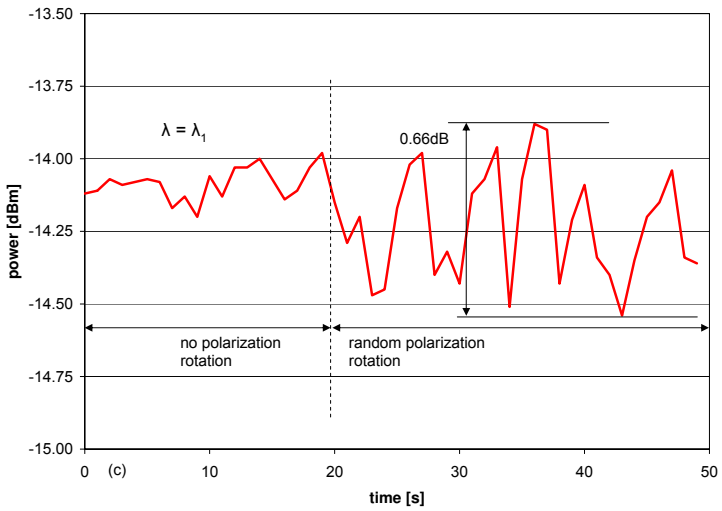

Fig. 9. Fluctuation in transmission over time when randomly varying the input polarization (starting at 20 seconds). The wavelength is kept constant at $\lambda = \lambda_1$ indicated in Fig. 8.

#78792 - $15.00 USD Received 8 January 2007; revised 9 February 2007; accepted 9 February 2007

6.2. *Improving the PDL*

While the 2-D fiber couplers make it possible to make a polarization-independent circuit, it proved not to be straightforward to obtain a low value of PDL. 1-D fiber couplers, which work only for a single polarization, are fairly alignment tolerant [14], but this is less the case for the 2-D gratings. It requires multiple alignment steps with different input polarizations to get a balanced incoupling in both waveguides, and thus polarization independence.

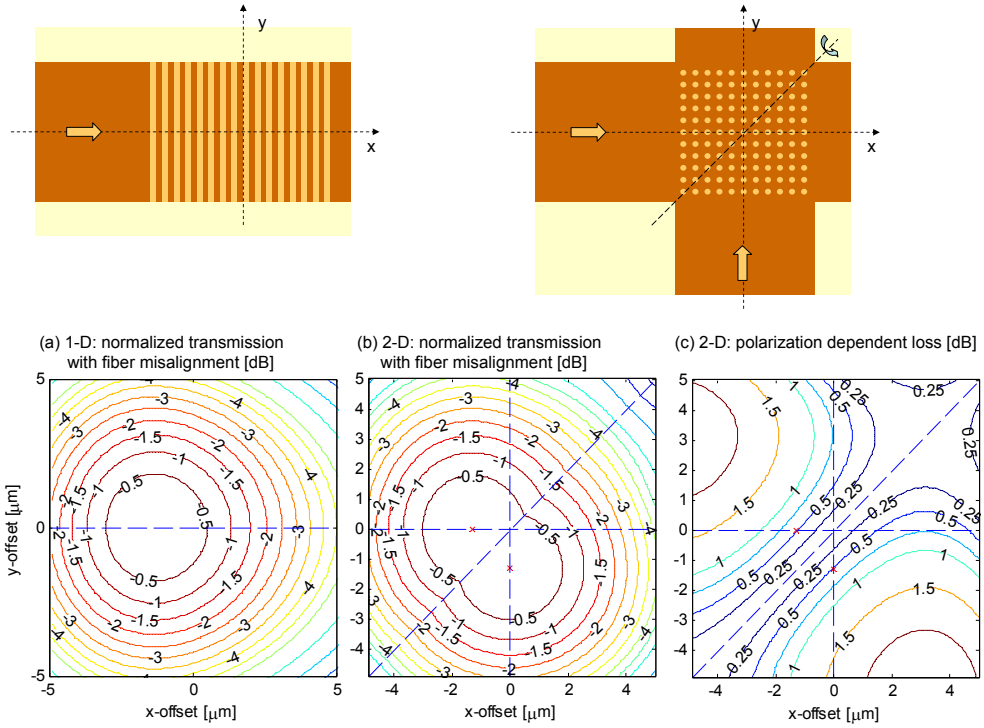

Fig. 10. Simple model of the coupling efficiency of a grating fiber coupler as a function of fiber position. (a) Transmission of a 1-D grating coupler due to fiber misalignment, normalized to the maximum transmission. (b) Normalized transmission of a 2-D grating coupler, after optimizing the polarization for each fiber position. (c) Polarization dependent loss (PDL) of a 2-D coupler for each fiber position.

The reason for this difficult alignment can be attributed to an non-optimized grating design: For these gratings the fiber positions with maximum power coupling do not lie on the symmetry axis of the grating. This way, it is not possible to minimize the PDL by maximizing the transmission of the circuit (either for a fixed polarization or by optimizing the polarization in each point). We explain this in a qualitative way in Fig. 10, using an approximate model. For a 1-D coupler, as shown in Fig. 10(a) , the coupling efficiency varies as a function of the position of the fiber along the axis of the waveguide [14, 12]. For the ease of calculation, the fiber is considered to be vertical. We calculated this by approximating the fiber mode as a Gaussian, and the light coupled from the grating as an exponential decaying mode profile, with the decay length determined by the coupling strength of the grating. The overlap between these approximate modes gives the coupling efficiency, which is calculated for various positions of the fiber. In Fig. 10(a) we have plotted the coupling loss of a 1-D grating, normalized to maximum coupling efficiency, as a function of fiber position. Of course, the position of maximum coupling

#78792 - $15.00 USD Received 8 January 2007; revised 9 February 2007; accepted 9 February 2007

efficiency depends strongly on the coupling strength of the grating.

In our simplified model, we treat the 2-D grating as a superposition of two of these 1-D gratings with the output waveguides at a right angle. For this, the fiber is considered to be vertical again. When the fiber is positioned over the diagonal axis of symmetry of the grating, the incoupling is balanced, and we should observe no PDL. In Fig. 10(b) we plotted the coupling efficiency in each position, when optimizing the polarization for each position. We can see that the positions of maximum incoupling (which lie on each waveguide axis) do not coincide on the diagonal. This results in a PDL in these positions, as the high coupling efficiency is only achieved for one fiber polarization. The PDL is plotted in Fig. 10(c).

The solution to this problem is to modify the grating design in such a way that the positions of maximum incoupling efficiency coincide and lie on the symmetry axis of the coupler grating. Not only should this facilitate alignment, but it should also improve alignment tolerances and coupling efficiency for polarization independent operation. In this example, where the maximum power coupling occurs before the light reaches the symmetry axis, the grating should be modified to reduce the coupling strength, at least at the start of the grating. This way, the position of maximum coupling is pushed further towards the symmetry axis. Even better, by using a variable coupling strength, it is possible to increase the efficiency of the grating, as has already been demonstrated in Ref. [12]. For the best results, the design should be done on the entire structure through numerical optimization, taking into account the exact fiber and waveguide angles. Future experiments are planned to implement this optimization.

7. Conclusion

We have demonstrated the first polarization-diversity circuit in SOI nanophotonic waveguides, in the form of a very compact, polarization-independent wavelength duplexer. Using a 2-D fiber coupler grating, it is possible to couple from standard single-mode fiber to SOI waveguides while simultaneously decompose the variable fiber polarization into separate circuits. Polarization independent behavior is achieved by propagating both polarizations through the same AWG in opposite directions. This way, the circuits for both polarization make use of the same wavelength-dependent element, obviating the need for local active tuning to align the transmission spectrum of both circuits. Measurements show well-defined bands for upstream and downstream traffic matching the simulation results. Insertion loss is between $-2.1\,dB$ and $-6.9\,dB$, intra-band non-uniformity is $4.8\,dB$ and crosstalk $-15\,dB$. When accurately aligning the fibers, we demonstrated a very low polarization dependent loss of only $0.66\,dB$.

Acknowledgments

This work was partly supported by the European Union through the IST-ePIXnet Network of Excellence and the Silicon Photonics Platform, and partly supported by the Belgian IAP-PHOTON project.

W. Bogaerts acknowledges the Flemish Fund for Scientific Research (FWO) for a post-doctoral grant. P. Dumon and Dirk Taillaert thank the the Flemish Institute for the industrial advancement of scientific and technological Research (IWT) for a specialization grant and a post-doctoral grant, respectively.

The authors would like to thank Johan Wouters, Patrick Jaenen and Stephan Beckx in IMEC for the process development, Johan Mees for the mask design and the people of the P-line for the actual processing. Also, Jonathan Schrauwen, Liesbet Van Landschoot and Frederik Van Laere are to be thanked for the SEM imaging.

#78792 - $15.00 USD Received 8 January 2007; revised 9 February 2007; accepted 9 February 2007